IOSR Journal of Mechanical and Civil Engineering (IOSR-JMCE)
e-ISSN: 2278-1684,p-ISSN: 2320-334X, Volume 20, Issue 4 Ser. II (July. – August. 2023), PP 26-39
www.iosrjournals.org

Cyclic Performanceof Extended End-Plate Beam-Column Steel ConnectionsUsing 3D Finite Element Models

Hassan Salama[a] and Mamoun Alqedra[b]
[1](*University College of Applied Sciences-UCAS, 1415 Gaza, Palestine)*
[2](*Civil Engineering Department, The Islamic University of Gaza, The Gaza Strip, Palestine)*

Abstract:
Extended End-Plate steel beam-to-column connections are widely used as moment resisting connections. Most of these connections are considered semi-rigid connections. This paper presents the behavior of Extended End-Plate (EEP) steel connections under cyclic loading by developing a three-dimensional nonlinear finite element (FE) model. ABAQUS software is utilized to develop the FE model and perform numerical analysis. Numerical modelling of the EEP connection was several parameters including: components geometry, material properties, load pattern, boundary condition, interaction and contact between connected parts, and analysis type. The FE models of EEP connections showedan excellent agreement with experimentally tested results in terms of the ultimate moment, hysteretic curves and failure modes. The verified FE model is then utilized to perform a parametric study to identify the EEP behavior under varying bolt diameter, head plate thickness, head plate stiffener, and beam flange.The failure modes, ultimate moment and hysteretic behavior were compared. The results indicated that increasing bolts diameter and head plate thickness enhance the EEP behavior in terms of strength, ductility, and rigidity with varying percentages. The existence of a head plate stiffener (HPS) increases the ultimate moment of EEP connection and prevents welding failure. Further, enlarging the beam section with and without HPS resulted in an increase in the ultimate moment and initial stiffness of the EEP connection. In addition, the moment rotation curves of EEP connections under monotonic loading are acting as a backbone curve for the moment rotation hysteretic curves under cyclic loading.

Keywords:*Extended End Plate connection; beam-column connection; Finite element modelling; Cyclic load.*

Date of Submission: 01-08-2023 Date of Acceptance: 10-08-2023

I. INTRODUCTION

End-plate connections have been extensively utilized in steel structures since the 1950s owing to their swift erection and straightforward fabrication, making them a popular choice for semi-rigid bolted steel connections in various applications. [1-5]. The end-plate connection consists of a head plate shop welded to the end of a beam and field-bolted to the connecting member. End-plate connections are still preferred in semi-rigid steel connections due to their high ductility and energy dissipation abilities when exposed to gravitational monotonic loading alongside lateral or vertical cyclic excitations [6-10].

Connections in the steel frame during earthquakes are subjected to relatively large cyclic rotations, which can affect the overall behavior of the connections [11]. Several experimental studies have investigated the behavior extended end-plate steel (EEP) connections under cyclic loading. [12] tested seven full-scale specimens of EEP connections under cyclic loading. They proposed qualitative design approach for seismic end-plate connections which could limit the deformation of the connection and yielding of its components. [13] tested two types of EEP connections (four-bolt unstiffened and eight-bolt stiffened) under cyclic loading, in which they showed that the two types of EEP connections could be used in seismic -resisting moment frames with required strength, stiffness, and ductility. [14] conducted experiments of eight specimens of end-plate connection under cyclic loading with different variablesparameter value as head plate thickness, bolt diameter, column web stiffener, and head plate stiffener. They proposed three failure mode requirements and recommended a calculation method to provide enough joint rotation capacity, energy dissipation capacity and ductility under earthquake loading. A group of eight full-scale structural steel beam-to-column end-plate moment connection specimens was tested under cyclic loads by [15]. The examined parameters in their study comprised end-plate thickness, bolt diameter, end-plate extended stiffener, column stiffener, type of flush and extended endplate. The results of these tests were moment capacity, rotational stiffness, rotation capacity and

hysteretic curves, which indicated that extended end-plate connections have adequate strength, joint rotational stiffness, ductility and energy dissipation capacity required for use in seismic moment frames.

(Tartaglia, R., et al., 2018) compared the effectiveness of the design and detailing criteria of the extended stiffened end plates connections of both American Institute of Steel Construction (AISC) requirements and the European project EQUALJOINTS funded by European Convection for Construction Steelworks (ECCS) to prequalify steel joints under seismic loading through conducting a parametric study utilizing a validated finite element model. The study revealed that there are differences in terms of ductile response in case of excessive loading of the connected beam, internal distribution of compression forces into the connections, geometrical imperfections, behavior of the joints under column loss. [17]tested several bolted stiffened end-plateand bolted flange-plate connections under cyclic loading using European hot-rolled profiles and built-up profiles and designed according to FEMA-350. The failure modes, hysteretic curves, ultimate moment and rotation values and panel zone extensions highlighted that using such connections does not affect its global behavior. [18] carried out a testing program on the cyclic characteristics of eight full-scale unstiffened extended end-plates with variable parameters. The specimens were under the 2010 AISC seismic provision loading protocol. All unstiffened extended end-plate were not able to develop full inelastic capacity of connected beams. [4] tested experimentally three full-scale bolted stiffened end-plate moment connections designed according to AISC to obtain the influence of bolt pretension levels under SAC cyclic-loading protocol. They found out that the pretension from the snug-tightened to fully pretensioned according to AISC and up to ultimate strength level has a denoting improvement on moment capacity, ductility of connection, energy absorption, elastic rotational stiffness, and improved behavior of bolts of connections.

Finite Element (FE) analysis can predict the connection behavior under different loads and configurations to an acceptable accuracy level. Using FE in modelling and analyzing the steel connections saves cost and expensive time of experimental work and effectively avoid uncontrollable errors during test processes [19]. [1] developed three FE models including welded connection, EEP connection, and flush end-plate connection using ABAQUS software to investigate the behavior of these connection types under cyclic loading. The proposed FE models were verified by typical quasi-static tests of end-plate connections, including both hysteretic curves and failure modes. The verified models pointed out that the connection methods (welded or bolted) could substantially affect the cyclic behaviors and in the high seismic zones, hysteretic behaviors, failure modes and seismic ductility should be considered thoroughly to select the suitable connection methods. [20] conducted a parametric study on the behavior of extended end-plate bolted connections under monotonic and cyclic loading using 3D nonlinear finite element analysis including shear force, diameter of bolt, thickness of head plate, and the effect of using head plate stiffener. The effect of shear force on the moment rotation relation and the stiffness of the connections was focused on and found to have has a significant effect on the connection stiffness. [5] applied finite element (FE) method to study the behavior of the semi rigid connections extended end-plate bolted beam-column connections subjected to column top-side cyclic loading. Their results of the parametric study pointed out that the panel zone shear force has a significant effect on the connection stiffness, and therefore, the initial stiffness calculation model under column top-side cyclic loadings is established. [6] reviewed the performance of semi-rigid steel connections under monotonic and cyclic loadings including extended end plate beam-column connections under both monotonic and cyclic loads. The reviewed papers revealed that extended end plates beam-column connections without stiffeners can offer semi-rigid connection having the maximum rigidity and resistance. Further, the review indicated that finite element analysis is still needed to examine the rotational behavior of connection and the application of three dimensional elements allows for simulating complex phenomena such as contact, plasticity, large deformations, and large displacements. [10] investigated the behavior of bolted extended end-plate beam-to-column connections numerically by finite element models subjected to cyclic loading comprising European I-Shape beams which do not satisfy the geometric requirements specified for seismic application in accordance with AISC 358-16. The developed finite element models were verified based on the results of previous experimental studies.

Comprehensive numerical and experimental programs on unstiffened extended end-plate connections having thin plates and large sized bolts under cyclic and monotonic loading to analyze the effects of several variables influencing the capacity of such connections were carried out by [21]. Their findings highlighted that thin end-plates can exhibit high ductility and strength; the design methods according to AISC 358-16 and EN1993-1-8 conservatively predict the plastic moment capacity of such connections. Accordingly, [21] presented an expression for the observed yield line pattern to estimate the plastic moment capacity more correctly.

The above-reviewed literature indicates that the modelling and behavior of the EEP connection under cyclic loading are complex in nature, with many varying parameters that affect its behavior. Consequently, there is a continuous need to obtain more accurate understanding of the behavior of such types of connections. Verified numerical simulations and their potential to conduct comprehensive parametric studies would substantially facilitate approaching this goal. The current study came in this context to develop a non- linear 3D FE model to

simulate the cyclic behavior of EEP steel connections using the ABAQUS [22]. The developed FE simulations were validated based on seven EEP connections, previously tested by [15]. The second objective of this study is carrying out a parametric study on EEP connections under cyclic loading using the verified 3D FE model. A comprehensive parametric study was carried out to obtain the influence of several parameters, including beam flange, head plate thickness, bolts diameter, and head plate stiffener. The failure modes, ultimate moment and hysteretic behavior are compared and thoroughly discussed. Finally, the (M–θ) hysteretic curves under cyclic loading for the same EEP connections are presented.

II. FINITE ELEMENT MODELLING

ABAQUS®is utilized to develop the FE model and perform numerical analysis. Numerical modelling of the EEP connection is performed by using the following parameters: components geometry, material properties, load pattern, boundary condition, interaction and contact between connected parts, and analysis type. The following subsections present more details about the FE modelling process.

Model description

The proposed FE model of the EEP connection is a T-shaped exterior connection of a steel frame, which comprise a column, beam, head plate, bolts, head plate stiffeners, and column stiffeners as shown in Figure 1. The head plate is welded to the end of the beam and fixed to a column by eight high strength bolts, as shown inFigure 2.

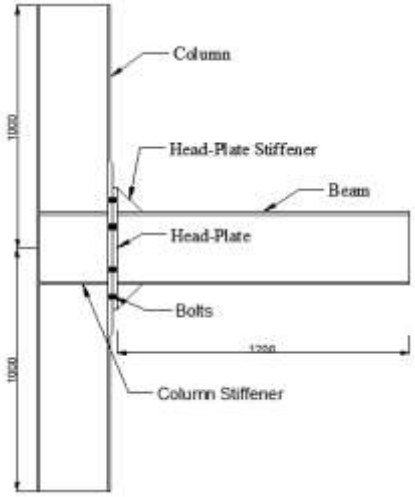

Figure 1. Examined model of EEP connection

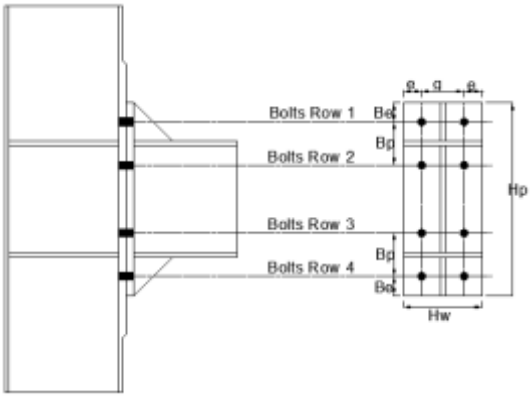

Figure 2. Geometrical details of the studied EEP connection

Material modelling

Steel yielding is modelled using the Von-Misses yield criteria with kinematic hardening. The bilinear elastic-plastic stress-strain curve is modelled in ABAQUS for all steel profiles and plates, as shown in Figure 3(a), while the trilinear elastic-plastic stress-strain curve is chosen for bolts, as shown in Figure 3(b).

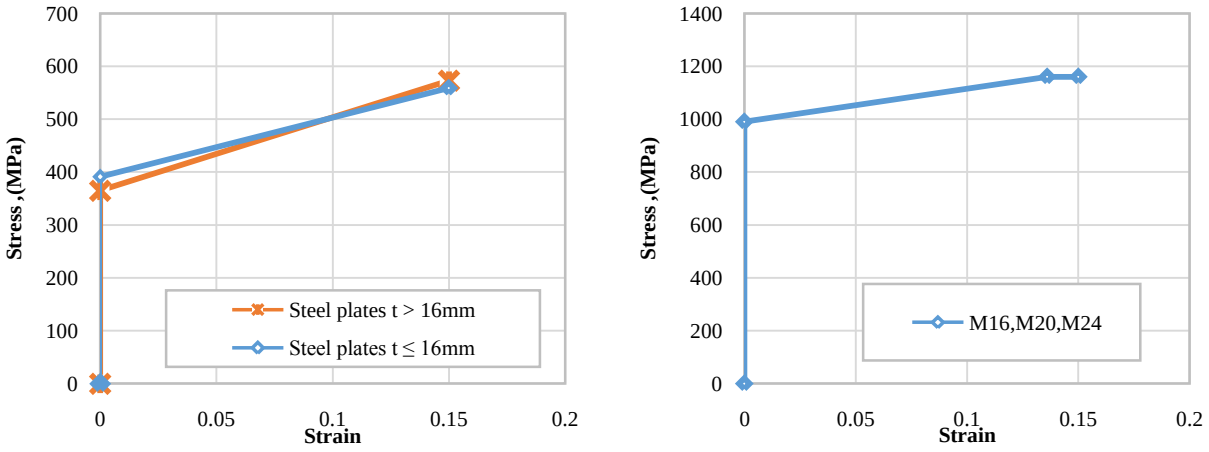

(a) steel profiles and plates (b) steel bolts

Figure 3. Stress-strain curves adopted in the FE model for (a) steel profiles and plates (b) steel bolts.

Element Types and Meshes

The 3D solid shape is applied to define all adopted EEP model parts (column, beam, head plate, bolts, head plate stiffeners, and column stiffeners), as shown in Figure 4comprising (a) Modeling of EEP components, (b) FE meshing of the model.Element (C3D8I) with an integration technique is adopted for meshing of all parts of the EEP connection under cyclic loading. This is recommended by several studies reported in the literature [1, 16, 23, 24] who selected the (C3D8I) element from the ABAQUS library for all EEP model parts (column, beam, head plate, bolts, head plate stiffeners, and column stiffeners). The full documentation of this element is included in [22]. In the current FE modelling, two meshing systems were applied, namely: a fine mesh in high-stress regions and a coarser mesh in the remaining areas.

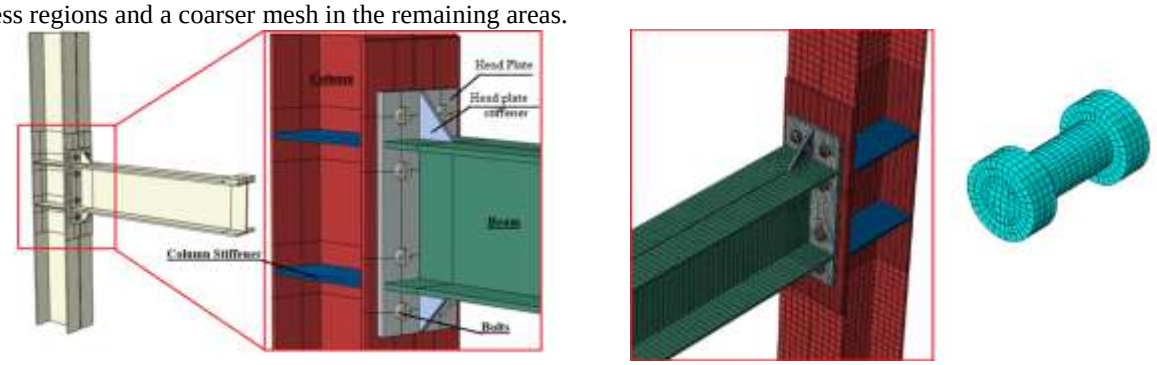

(a) Modeling of EEP components (b) FE meshing of the model

Figure 4. Element modelling: (a) Modeling of EEP components, (b) FE meshing of the model

Constraints Modeling

Modelling the EEP connection components' constraints is one of the most critical processes, which significantly influence the numerical results. Tie and contact constraints are adopted in the EEP connection to simulate the welded and bolted connection, respectively. Contact constraints represent the contact surfaces between head-plate/column flange, bolt screw/hole, nuts/column flange, and nuts/head-plate, as shown in Figure 5 (a) and (b). The contact surface properties are defined as tangential behavior using "penalty stiffness formulation" and Normal behavior using "hard" contact. The friction coefficient is obtained from the experimental data [15].

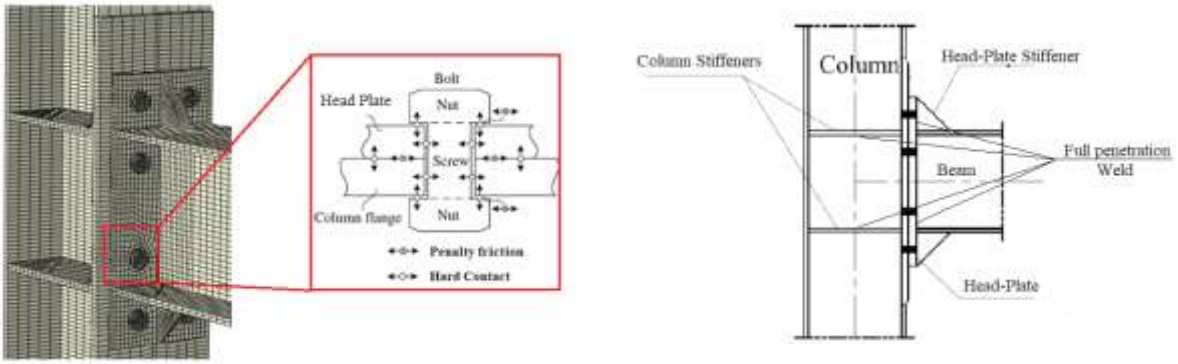

(a) Contact constraint for Bolted connection (b) Tie constraints for Welded connection

Figure 5. Constraints between EEP connection components for (a) Contact constraint and (b) Tie constraints.

Tie constraint is utilized to represent the full penetration weld behavior, which is applied to connect the beam and head plate; head plate stiffeners and head plate; stiffness plates and column as shown in Figure 5(b). More details on modelling contact and tie constraints can be found in [22].

Boundary Conditions and Loadings

Two different types of boundary conditions are utilized in the developed EEP connection FE model. Both ends of the column are restrained in the three directions (*x*, *y*, and *z*) for all the translational and rotational degrees of freedom, as shown in Figure 6. Constraints in one direction (*x*) are added at the end of beam flanges to avoid the lateral-torsional buckling. The cyclic load is introduced at the end of the beam flange as a vertical displacement based on load-time history to define the direction of this displacement as shown in Figure 7. The pretension loads are initially applied to the bolts as a first step.

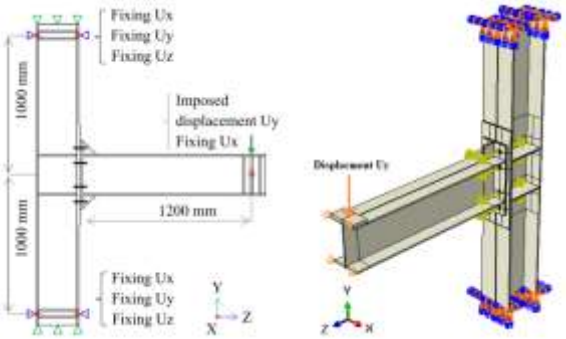

Figure 6. Boundary conditions and loading of EEP connection

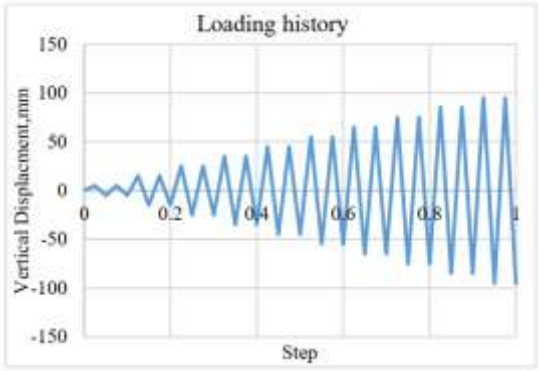

Figure 7. Load-time history for cyclic load

Analysis Type

The Dynamic Implicit analysis is carried out to analyze the FE models using the ABAQUS/Standard solver. The maximum number of increments, which is performed in defining the analysis step is 1000 increments. The selection of this number of increments (1000) was achieved based on preliminary analysis runs until reaching the optimum number of increments. The initial increment size is 1%, and the maximum is 5% of applied displacement to obtain good accuracy and reasonable run time.

III. VERIFICATION OF THE DEVELOPED FE MODEL

The verification of the developed FE models is conducted by comparing the obtained results with the corresponding results measured experimentally from seven specimens of EEP connections tested by [15]. The same specimen's geometry, material properties, and test procedure of the experimental works of [15] were applied to define the proposed FE models in order to compare and validate the obtained results.

Description of the examined EEP configurations

The studied configurations of EEP connections are presented in **Table 1**, which were chosen from the work of [15]. The column and the beam sizes are listed in **Error! Reference source not found.**2. The thickness

of the column stiffeners are 12 mm and 10 mm for head plate stiffeners. The column flange thickness equals the head plate thickness within 100 mm above and below the head plate to avoid column flange failure. The bolt hole diameter is 2.0 mm larger than the bolt diameter. The contact surfaces' friction coefficient between the head plate and the column flange is taken as 0.44.The yield strength (f_y), the ultimate strength (f_u), and Young's modulus (E) of the EEP connections' components are obtained from [15]test and listed in **Error! Reference source not found.**. Poisson's ratio is assumed (0.3).

Table 1: Examined configurations of EEP connections (Shi, Shi et al. 2007).

Test No.	Head plate thickness HP_{thick}, mm	Bolt diameter $b_{dia,}$ mm	Column Stiffener, CS	Head plate stiffener, *HPS*
JD 02	20	20	Yes	Yes
JD 03	20	20	Yes	No
JD 04	20	20	No	Yes
JD 05	25	20	Yes	Yes
JD 06	20	24	Yes	Yes
JD 07	25	24	Yes	Yes
JD 08	16	20	Yes	Yes

Verification Process

The Verification process of the developed FE model is examined by comparing the obtained numerical results with the corresponding results measured from the performed experiments. The moment is obtained by multiplying the applied force by the lever arm, which is the distance between the loading point to the column flange (1200mm in this study). The joint rotation is the relative rotation of the centerlines of the beam flanges at the beam end, which includes two parts: The shearing rotations (θ_s), contributed by the column panel zone; and the gap rotation (θ_{ep}), caused by the relative deformation between the head plate and the column flange including their bending deformation as well as the extension of the bolts, as indicated in Figure 9. The shearing rotation (θ_s) is calculated by (Δ/h_f), and the gap rotation (θ_e) is calculated by (δ/h_f), and the total $\theta = (\theta_s+\theta_e)$.

Table 2: Dimensions of column and beam cross-sections (Shi, Shi et al. 2007).

	Web depth, w_d	Web thickness, w_t	Flange width, f_w	Flange thickness, f_t
Beam, mm	300	8	200	12
Column, mm	300	8	250	12

Table 3:Material properties (Shi, Shi et al. 2007)

Material	Yield strength (f_y). MPa	Ultimate strength (f_u), MPa	Young's modulus (E), MPa)	Bolt pretension force, kN
Steel profile ≤16mm	409.0	536.6	195 452	-
Steel profile >16mm	372.6	537	188 671	-
Bolts (M20)	995	1160	206000	199
Bolts (M24)	975	1188	206000	283

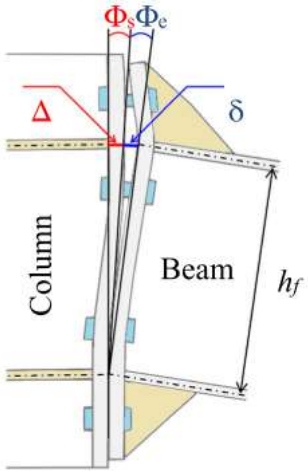

Figure 8. Joint rotation (θ) in terms of shearing and gap rotation Verification Outputs

Verification of the developed FE model is examined by comparing the obtained numerical results with those of the experiments in terms of the ultimate moment, the (M–θ) hysteretic curve, and the connection's failure mode, as described in the following sections.

Ultimate Moment

The ultimate moments obtained from the developed FE models indicate excellent agreement with the corresponding values measured by [15], as presented in Table 4: Comparison between numerical and experimental results: ultimate moments

The slight difference between the FE model values and the experiments are attributed to several factors, such as material properties and contact surfaces approximation in the FE models and those of the actual values.

Table 4: Comparison between numerical and experimental results: ultimate moments

Test No.	Mu experiments, *kN.m*	Mu FE models, *kN.m*	Ratio (Experiments/FE)
JD 02	320.1	337.7	0.95
JD 03	288.4	297.80	0.97
JD 04	289.4	291.67	0.99
JD 05	331.4	350.44	0.95
JD 06	336.2	375	0.90
JD 07	364.0	365	1.00
JD 08	283.5	306.25	0.93

M–θ hysteretic Curves

Figure 9 highlighted an excellent correlation between the (M–θ) hysteretic curves of the FE models compared with those measured from the EEP connection tests, which ensure the capability of the developed FE models.

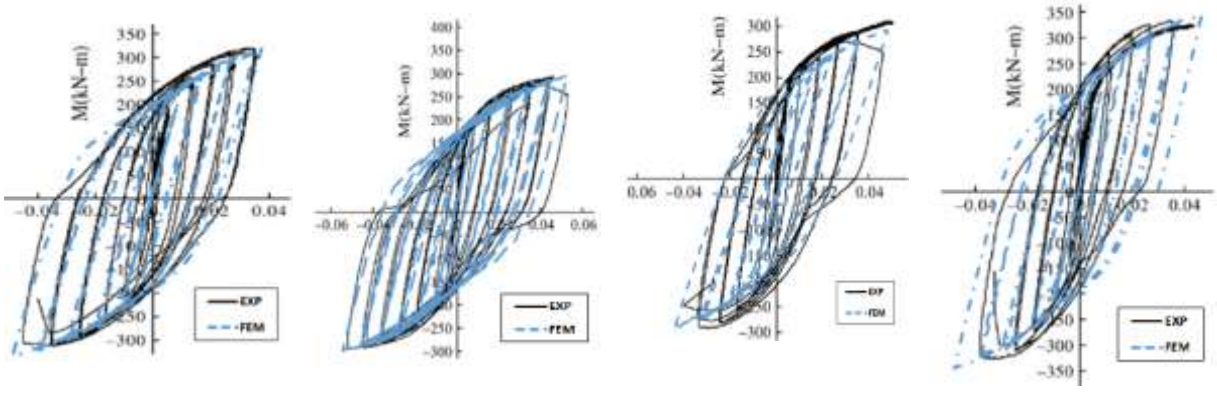

(a): JD 02 **(b):** JD 03 **(c):** JD 04 **(d):** JD 05

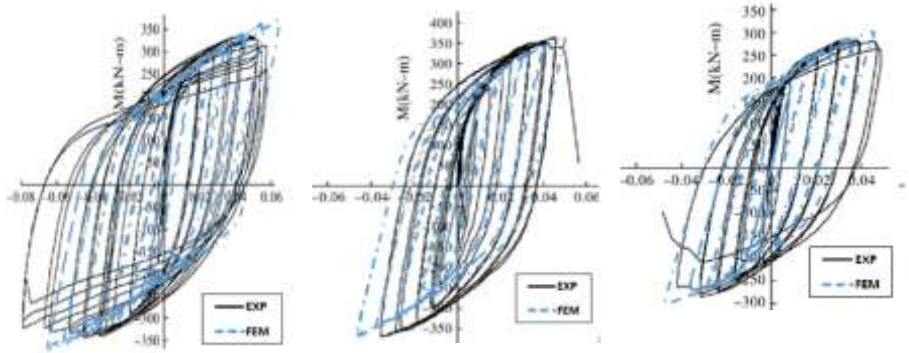

(e): JD 06 **(f):**JD 07 **(j):** JD 08

Figure 9. Comparison of the FE model and experiment results:(M–θ) hysteretic curves

Failure Modes

The resemblance between the failure modes observed in the experimental tests and those obtained by the current numerical simulation of FE models are presented in Figure 10. The comparison shows excellent results in simulating the final failure modes of the experimental tests.

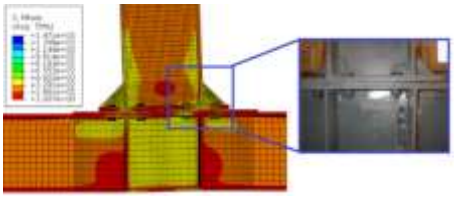

(a): JD02 (Bolt rupture)

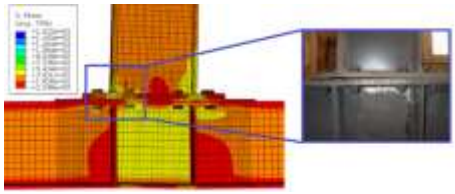

(b): JD03 (Bolt rupture and head plate yielding)

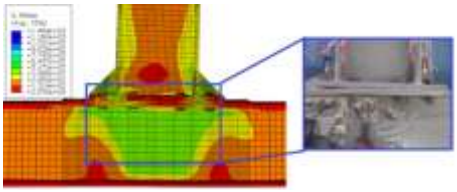

(c): JD04 (Column web buckling and bolt rupture)

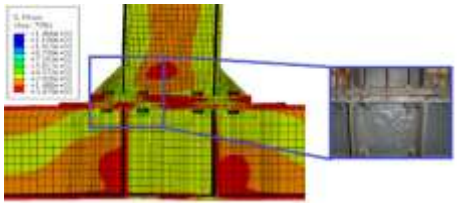

(d):JD 05 (Bolt rupture)

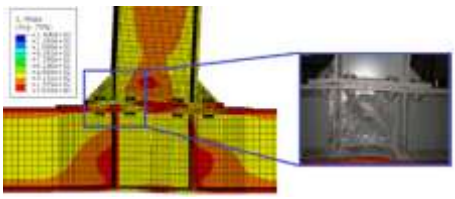

(e): JD06 (Head plate stiffener fracture and column flange buckling)

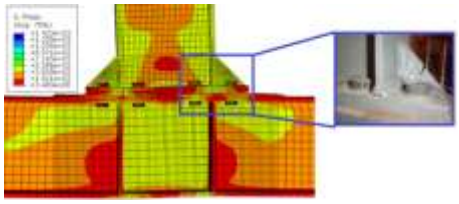

(f): JD07 (Head plate stiffener fracture)

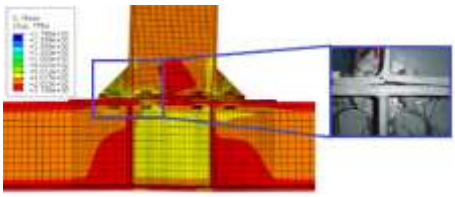

(g): JD08 (Head plate stiffener fracture, and bolt rupture)

Figure 10. Comparison of the FE model and experiment results: failure modes for tests from JD02 to JD08

The verification process proved that the developed 3D FE model successfully simulates the EEP connection's behavior under cyclic loading as per the excellent correlation between numerical and experimental results. Consequently, a parametric study was performed to investigate the effect of several design variables on the bahavior of the EEP connections.

IV. PARAMETRIC STUDY

Several parameters are investigated to determine its influence on EEP connection behavior using the verified 3D FE models, namely: beam flange (b_f), head plate thickness (hp_{thick}), bolts diameter (B_{dia}), and head plate stiffener (***HPS***). Table 5 and 6 present the fixed parameters at specific levels and the varying parameters of the EEP connection components, respectively. The steel material properties used to define the FE model for the parametric study are considered similar to those applied by [15] experiments. The value of bolts pretension in the FE model was considered according to [25].

Table 5: Constant parameters of the FE model components

Parameter	Value (mm)
Beam web width and thickness, (b_{ww}, b_{wt})	300,8
Beam length, (b_L)	1200
Column flange width and thickness, (c_{fw} , c_{ft})	300, 10
Column web width and thickness, (c_{ww} , c_{wt})	250, 12
Column length, (c_L)	2000
Head Plate length, (hp_{length})	500
Head plate width, (hb_{width})	200

Table 6: Varying parameters of the FE model components

Parameter	Value
Head Plate thickness (hp_{thick}), mm	$hp_{thick,1}$=16, $hp_{thick,2}$ = 20, $hp_{thick,3}$=25
Beam Flange (b_f), mm	$b_{f,1}$ = 200, $b_{f,2}$=150
Bolts diameter (b_{dia}), mm	$b_{dia,1}$ =16, $b_{dia,2}$ =20, $b_{dia,3}$=24
Head plate stiffener (***HPS***)	Y_{45}= with triangle stiffener. Y_{90}= with rectangular stiffener. ***NS*** = without stiffener.

V. ANALYSIS OF RESULTS

The analysis of 27 FE models of EEP connections subjected to cyclic loads is summarized in Table 7. It should be mentioned that FE analysis under cyclic loading is time expensive. It takes 10 hours to analyze a FE model of EEP connection on an ordinary computer.

Table 7: Parameters of the FE models under cyclic loading and their results

FE model	FE model parameter				Rotation Capacity (rad)	Ultimate Moment, kN.m	Location of Failure mode
	hp_{thick}	b_{dia}	b_f	*HPS*			
C1	16	16	200	Y_{45}	0.029	245.84	Beam Flange
C2	16	16	200	*NS*	0.028	201.78	Beam Flange
C3	16	20	200	Y_{45}	0.051	304.67	Head plate
C4	16	20	200	*NS*	0.041	250.80	Head plate welding & beam flange
C5	16	24	200	Y_{45}	0.055	318.78	Head plate
C6	16	24	200	*NS*	0.050	269.03	Head plate welding & beam flange
C7	20	16	200	Y_{45}	0.030	250.87	Beam Flange
C8	20	16	200	*NS*	0.028	219.13	Beam Flange
C9	20	20	200	Y_{45}	0.061	336.39	Beam Flange
C10	20	20	200	*NS*	0.053	286.75	Beam Flange
C11	20	24	200	Y_{45}	0.061	349.08	Beam failure
C12	20	24	200	*NS*	0.063	310.89	Head plate welding & beam flange
C13	25	16	200	Y_{45}	0.030	255.79	Beam Flange
C14	25	16	200	*NS*	0.035	244.51	Beam Flange
C15	25	20	200	Y_{45}	0.058	350.06	Beam Flange
C16	25	20	200	*NS*	0.053	308.82	Head plate welding & beam flange
C17	25	24	200	Y_{45}	0.052	360.90	Beam failure
C18	25	24	200	*NS*	0.053	321.97	Head plate welding & beam flange
C19	20	16	150	Y_{45}	0.029	247.30	Beam Flange
C20	20	20	150	Y_{45}	0.040	302.71	Beam failure
C21	20	24	150	Y_{45}	0.032	302.47	Beam failure
C22	25	16	150	Y_{45}	0.027	252.08	Beam Flange
C23	25	20	150	Y_{45}	0.032	309.06	Beam failure
C24	25	24	150	Y_{45}	0.030	312.65	Beam failure
C25	20	16	200	Y_{90}	0.030	255.00	Beam Flange
C26	20	20	200	Y_{90}	0.053	240.20	Beam Flange
C27	20	24	200	Y_{90}	0.0537	355.1868	Beam failure

Ultimate Failure Modes

The deformation shapes at ultimate failure modes of the studied EEP connections are illustrated in Figure 11. For EEP connections with larger bolt diameter of 20 and 24 mm as in (C4) models, the failure occurred in the welding between the beam flange and the head plate due to the absence of the head plate stiffener (***HPS***) as shown in Figure 11 (a). For thick head plate models of C15, the failure occurred in the beam, as shown in Figure (b), while for connections with a thin head plate as in models (C3), Figure 11(C) showed that the failure occurred in the head plate as shown in. In C19 models with a small bolt diameter of 16mm, the failure occurred in the bolts that reach ultimate strength and strain, as shown in Figure 11(d).

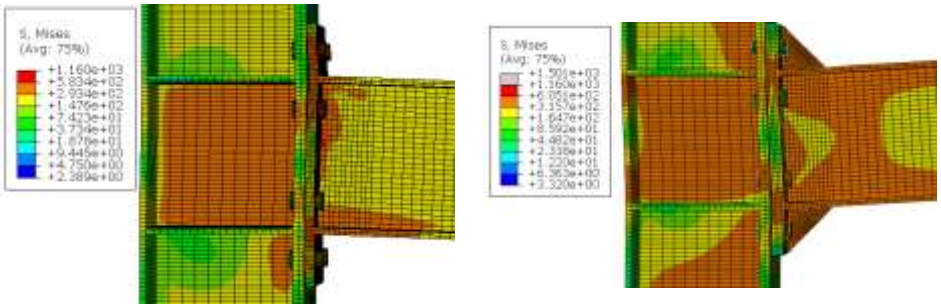

(a) C4 (b) C15

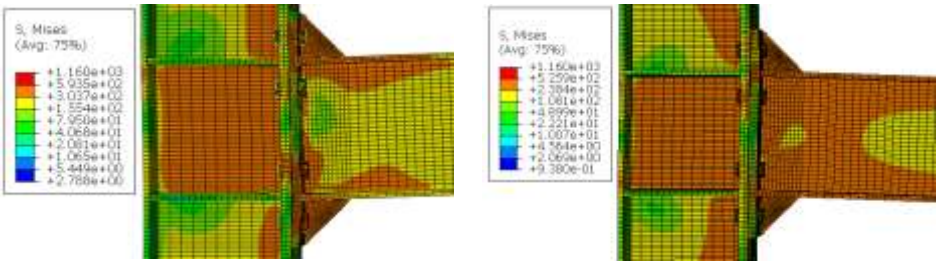

(c) C3 (d) C19

Figure 11. Failure modes of EEP connections resulted from FE analysis for FE model C3, C4, C15,C19

Effect of Bolt Diameter

Figure 12 displays the influence of three bolt diameters 16, 20, and 24mm on the ultimate moment, and the rotational capacity of the EEP connections with three values of head plate thickness, hp_{thick} 16, 20, and 25 mm with head plate stiffener ***HPS***. It can be noticed that increasing both bolt diameter, $b_{dia}$and head plate thickness (hp_{thick}) increases the ultimate moment and the rotation capacity with varying percentages.

As indicated in Figure 12(a), the EEP connections with ***HPS*** with bolt diameters ranging from 16 to 20 mm showed an increase in the ultimate moment by about 32%. However, using a bolt diameter of 20 to 24 mm increases the ultimate moment by only about 4%. From Figure 12(b), it can be noted that using a bolt diameter of 20 mm increases the rotation capacity by about 90%. While a slightly different value of the rotation capacity when using bolt diameter of 24 mm. On the other hand, using a head plate with a thickness of 25 mm leads to decreased rotation capacity.

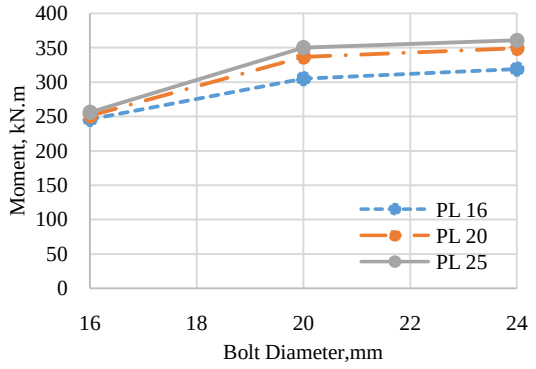

(a): Effect on the ultimate moment

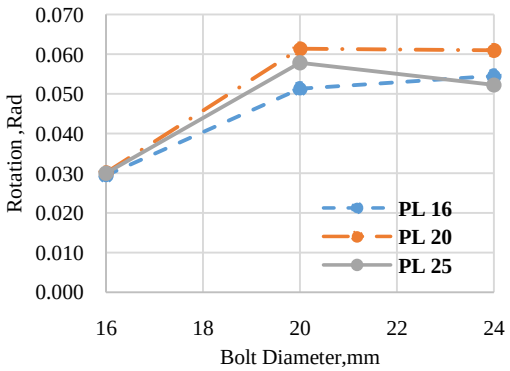

(b): Effect on the rotation capacity

Figure 12. Effect of bolts diameter for EEP with HPS on (a) the ultimate moment, and (b) rotation capacity

In comparison with the study carried out by ElSabbagh, A., Sharaf, T., Nagy, S., & ElGhandour, M. (2019), it was found out that increasing bolt diameter from 16mm to 24mm increased the ultimate load of both stiffened and unstiffened connections by approximately 15%. Furthermore, the ultimate load of unstiffened connections specifically was improved by approximately 21% when the bolt diameter was increased from 16mm to 24mm. According to Luo, Liang, et al. (2020), increasing the bolt diameter lead to higher ultimate flexural capacity and initial rotational rigidity in connections. Specifically, when the bolt diameter increases from 16 to 24 mm, the ultimate load value increases by 32.1% and 25.6%, respectively. Özkılıç, Yasin Onuralp (2023) indicated that the increase in the diameter of bolt and/or weld thickness outcomes in a rise in the plastic moment capacity.

Effect of head plate thickness

It can be seen that increasing the head plate thickness with/without HPS leads to an increase in the ultimate moment of EEP connections as shown in Figure 13. When using the head plate thickness of 20 mm, the ultimate moment for stiffened and unstiffened head plates increases by about 7% and 13%, respectively. In addition, when using the head plate thickness of 25 mm the ultimate moment of connection for stiffened and unstiffened head plate increases by about 3% and 8%, respectively.

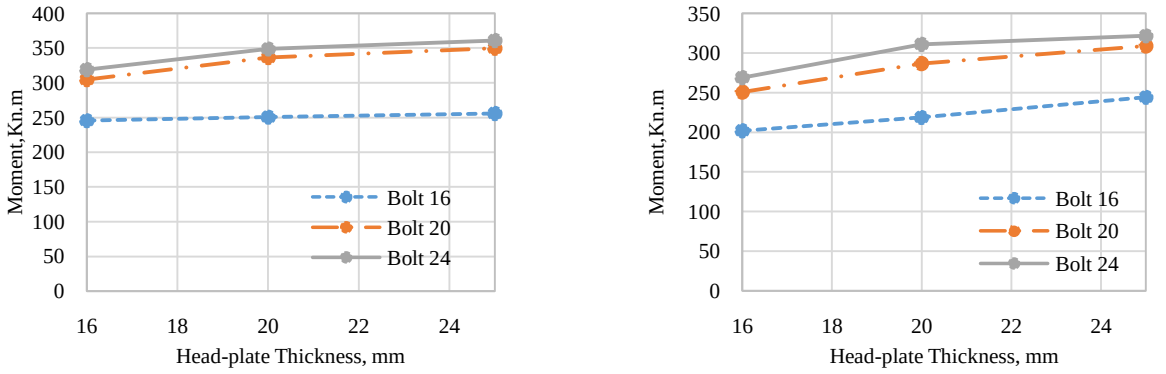

(a) with *HPS* (b) without *HPS*

Figure 13. Effect of head plate thickness on the ultimate moment for (a) with *HPS* and (b) without *HPS*

These results agree with the findings of ElSabbagh, A., Sharaf, T., Nagy, S., & ElGhandour, M. (2019) as they indicated that an increase in head plate thickness results in higher connection stiffness with varying values between about 4% and 15%. Further, Luo, Liang, et al. (2020) obtained similar findings with an enhancement ranged between 4% and 15% when enlarging the thickness of the head-end plate thickness.

Effect of Head Plate Stiffeners

As mentioned in the previous sections, using HPS in EEP connections increases their ultimate moment and rotation capacity. Further, using HPS prevents the failure of welding between the head plate and beam flanges. As illustrated in Figure 14, installing HPS increases the ultimate moment by about 10%, 15%, and 20% for the head plate's thickness 16, 20, and 25 mm, respectively. This finding allies with that of ElSabbagh, A., Sharaf, T., Nagy, S., & ElGhandour, M. (2019) who revealed that the head plate stiffener improves connection stiffness and ultimate rotation capacity. They concluded that the stiffeners can delay or prevent the failure of the head plate or the weld between the flange and the head plate.

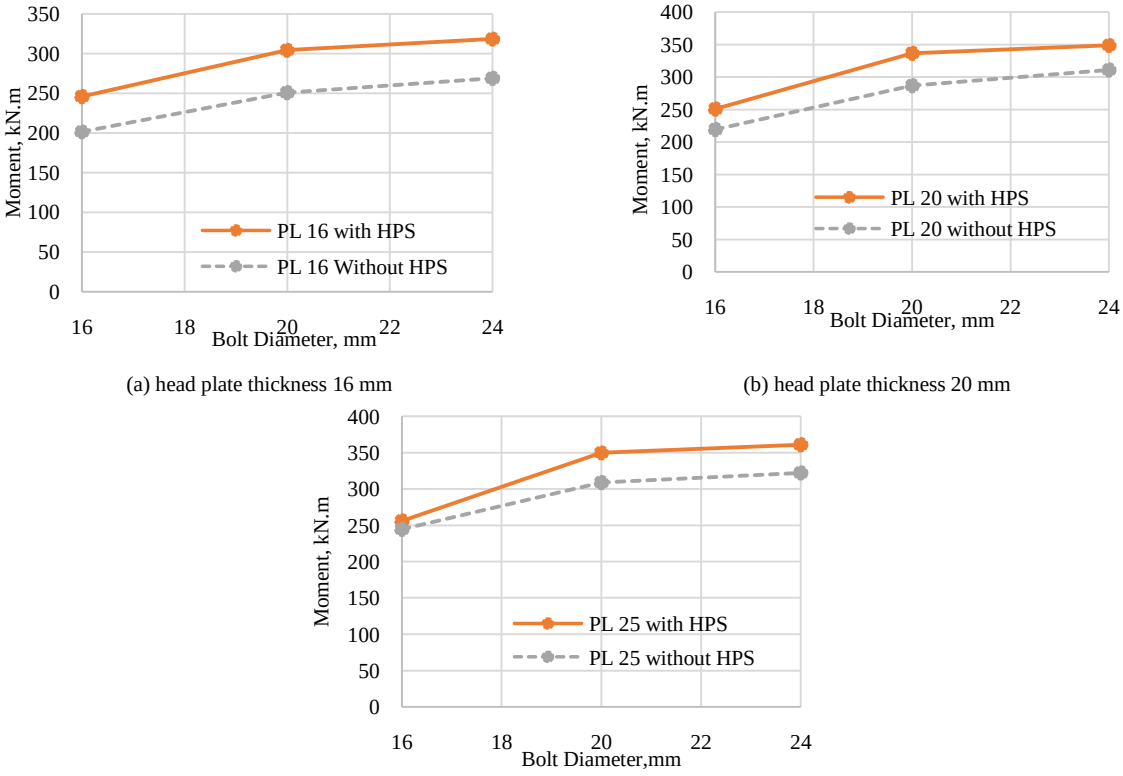

(a) head plate thickness 16 mm (b) head plate thickness 20 mm

(c) head plate thickness 24 mm

Figure 14. Effect of HPS on the ultimate moment for head plate thickness (a) 16 mm, (b) 20 mm and (c) 25 mm

Figure 15 remarkably revealed that changing the shape of the HPS from a triangle to a rectangle (Y45, Y90) does not affect the value of the ultimate moment of connection.

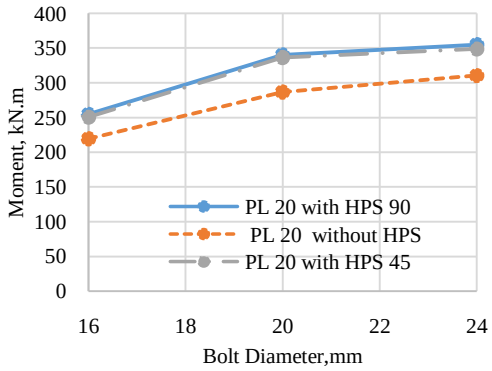

Figure 15. Effect of HPS shape on the ultimate moment

Effect of Beam Flange

The parametric study (through Table 8 and Figure 16) found out that utilizing a larger beam flange section with HPS leads to an increase in the ultimate moment. For EEP connections with bolts diameter of 16mm, a slight change in the ultimate moment's value has occurred. Changing the beam flange from 200 to 150mm for EEP connection with head plate thickness 20 and 25 mm the ultimate moment decreased for bolts diameter 16, 20, and 24mm by about 1.5%, 10%, and 13%, respectively as shown in Figure 16.

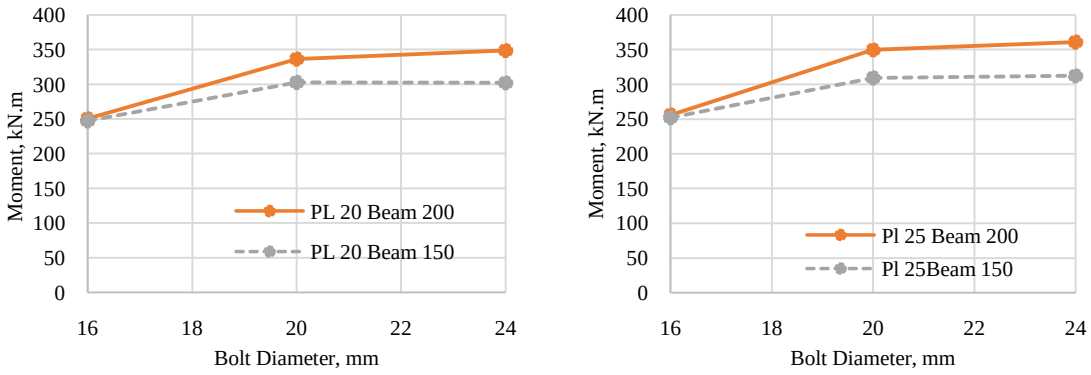

(a) Head plate thickness of 20 mm (b) Head plate thickness 25 mm

Figure 16. Effect of Beam flange on the ultimate moment for Head plate thickness of: (a) 20 mm and (b) 25 mm

In addition to that, varying the beam flange from 200 to 150mm resulted in a reduction in the rotation capacity of the EEP connection as presented in Figure 17. For EEP connection with head plate thickness 20 mm and bolts diameter 16, 20, and 24mm the rotation capacity is decreased by about 4%, 34%, and 48%, respectively. While for EEP connection with head plate thickness 25 mm with bolts diameter 16, 20, and 24mm the rotation capacity is decreased by about 10%, 45%, and 42%, respectively. Özkılıç, Yasin Onuralp (2023) indicated that the influence of enlarging the beam flange width led to the average of 11% improvement in the plastic moment capacity when using a beam flange larger than the head end plate with +25 mm, however, when installing beam flange width larger than 50 mm, only 2% of the plastic moment capacity was increased.

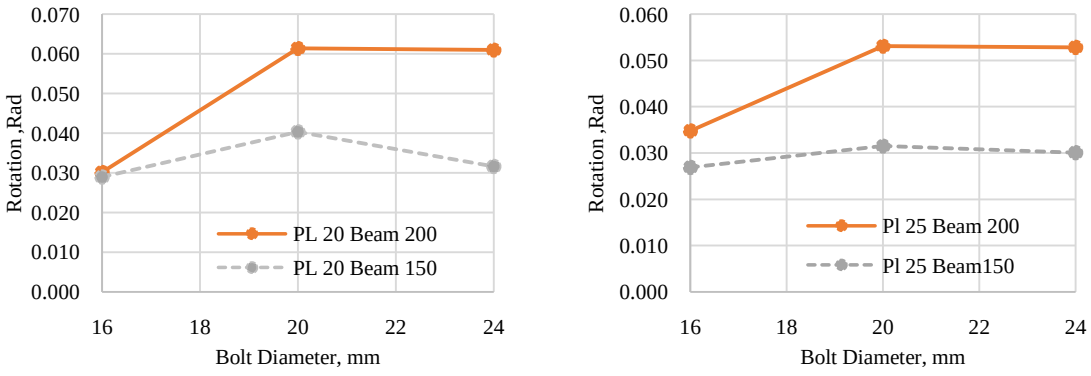

(a) Head plate thickness of 20 mm (b) Head plate thickness 25 mm

Figure 17. Effect of Beam flange on the rotation capacity for Head plate thickness of:
(a) 20 mm and (b) of 25 mm

(M– θ) Curves of Monotonic and Cyclic Loads

Figure 18 highlights that the (M– θ) curves for the same EEP connections under monotonic loading are acting as a backbone curve for the (M–θ) hysteretic curves of EEP connections under cyclic loading. These results indicate that the developed FE model represented the actual behavior of the proposed EEP connection under both monotonic and cyclic loading.

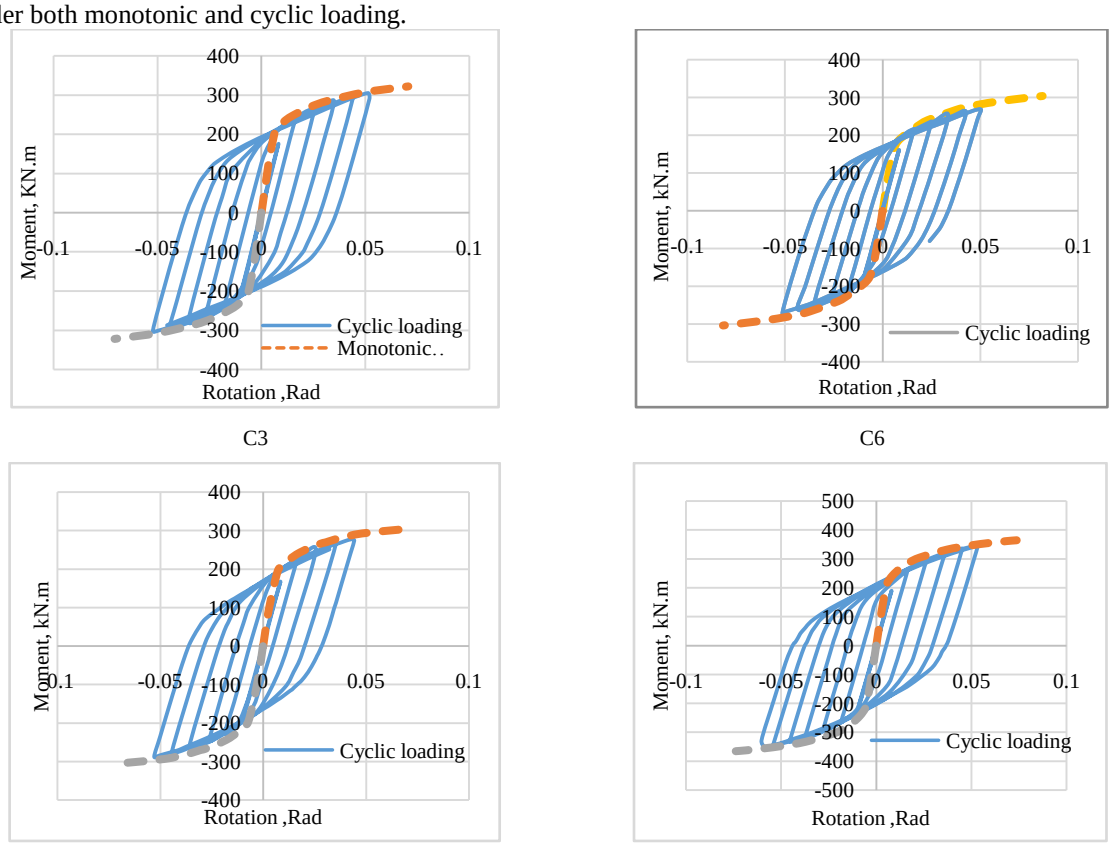

Figure 18. Comparison between (M–θ) curves under cyclic and monotonic loadings for the FE models: C3. C6, C10, C15.

VI. CONCLUSIONS

This study aims at studying the behavior of EEP connection under cyclic load by developing a 3D FE model using nonlinear FE analysis and conducted by ABAQUS software. Based on the study results, the following conclusions can be drawn:

1. The developed 3D FE models successfully simulate the actual behavior of steel EEP connections as compared with the results of the applied experimental works conducted.The FE models correctly simulates the final failure modes of the experimental tests.
2. Increasing both bolt diameter and the head plate thickness increases the ultimate moment, and the rotation capacity with varying percentages.
3. The EEP connections with HPS and bolt diameters ranging from 16 to 20 mm pointed out an increase in the ultimate moment by about 32%. However, increasing the bolt diameter beyond 20 showed an increase in the ultimate moment by only about 4%.
4. Using a bolt diameter of 20 mm increases the rotation capacity by about 90% with respect the 16mm bolt diameter. While a slight increase was noticed when using a bolt diameter of 24 mm. On the other hand, using a head plate with a thickness of 25 mm leads to decreased rotation capacity.
5. The ultimate moment increases by about 7% and 13% for stiffened and unstiffened head plates when using the head plate thickness of 20 mm, respectively. On the other hand, 25mm thick head plate illustrated an increase in the ultimate moment of connection by about 3% and 8% for stiffened and unstiffened head plate, respectively.

6. The results revealed that using HPS would enhance the ultimate moment by about 10%, 15%, and 20% for the head plate's thickness 16, 20, and 25 mm, respectively.
7. Changing the shape of the HPS from triangle to rectangle shape does not affect the value of the ultimate moment of connection.
8. The comparison of the obtained parametric behavior results with previous experimental and FE models pointed out that the developed FE models successfully simulate the overall performance of the EEP connections and can be applied to study other parameters.
9. The (M– θ) curves of FE models under monotonic loading are acting as a backbone curve for the (M–θ) hysteretic curves. These results indicate that the developed FE model represented the actual behavior of the proposed EEP connection under both monotonic and cyclic loading.

VII. REFERENCES

[1]. Wang, M., et al., Numerical study on seismic behaviors of steel frame end-plate connections. Journal of Constructional Steel Research, 2013. 90: p. 140-152.
[2]. Abdalla, K., G. Abu-Farsakh, and S. Barakat, Experimental investigation of force-distribution in high-strength bolts in extended end-plate connections. Steel and Composite Structures, An International Journal, 2007. 7(2): p. 87-103.
[3]. Bahaz, A., et al., Analysis of the Behaviour of Semi Rigid Steel End Plate Connections. MATEC Web Conf., 2018. 149: p. 02058.
[4]. Noferesti, H. and M. Gerami, Cyclic Behavior of Bolted Stiffened End-Plate Moment Connections for Different Bolt Pretensioning Levels: An Experimental Study. Shock and Vibration, 2023. 2023.
[5]. Luo, L., et al., Parametric Analysis and Stiffness Investigation of Extended End-Plate Connection. Materials (Basel), 2020. 13(22).
[6]. Al-Fisalawi, R.K., A.-H.L. Khalid, and M.K. Al-Kamal. Performance of semi-rigid steel connections under monotonic and cyclic loadings: a review. in IOP Conference Series: Materials Science and Engineering. 2021. IOP Publishing.
[7]. Herath, H.M.H.K., et al., Performance-based design method for bolted stiffened end-plate connection under monotonic loading. Structures, 2023. 53: p. 214-227.
[8]. Luo, L., et al., Parametric Analysis and Stiffness Investigation of Extended End-Plate Connection. Materials, 2020. 13(22): p. 5133.
[9]. Shaheen, M.A., A new idea to improve the cyclic performance of end plate beam–column connections. Engineering Structures, 2022. 253: p. 113759.
[10]. Yardımcı, S. and C. Vatansever. Nonlinear Behavior of Bolted Extended End-Plate Beam to Column Connections Subject to Cyclic Loading. in Building for the Future: Durable, Sustainable, Resilient. 2023. Cham: Springer Nature Switzerland.
[11]. Luo, L., et al., Seismic Behavior of Extended End-Plate Connections Subjected to Cyclic Loading on the Top-Side of the Column. Materials, 2020. 13(17): p. 3724.
[12]. Korol, R.M., A. Ghobarah, and A. Osman, Extended end-plate connections under cyclic loading: Behaviour and design. Journal of Constructional Steel Research, 1990. 16(4): p. 253-280.
[13]. Sumner, E.A. and T.M. Murray, Behavior of Extended End-Plate Moment Connections Subject to Cyclic Loading. Journal of Structural Engineering, 2002. 128(4): p. 501-508.
[14]. Guo, B., Q. Gu, and F. Liu, Experimental behavior of stiffened and unstiffened end-plate connections under cyclic loading. Journal of Structural Engineering, 2006. 132(9): p. 1352-1357.
[15]. Shi, G., Y. Shi, and Y. Wang, Behaviour of end-plate moment connections under earthquake loading. Engineering Structures, 2007. 29(5): p. 703-716.
[16]. Tartaglia, R., et al., Full strength extended stiffened end-plate joints: AISC vs recent European design criteria. Engineering Structures, 2018. 159: p. 155-171.
[17]. Yılmaz, O., et al., Experimental investigation of bolted stiffened end-plate and bolted flange-plate connections. Latin American Journal of Solids and Structures, 2019. 16.
[18]. Faridmehr, I., et al., Cyclic behaviour of fully-rigid and semi-rigid steel beam-to-column connections. International Journal of Steel Structures, 2020. 20: p. 365-385.
[19]. Lin, T., et al., Finite-Element Analysis of High-Strength Steel Extended End-Plate Connections under Cyclic Loading. Materials, 2022. 15(8): p. 2912.
[20]. ElSabbagh, A., et al., Behavior of extended end-plate bolted connections subjected to monotonic and cyclic loads. Engineering Structures, 2019. 190: p. 142-159.
[21]. Özkılıç, Y.O., Cyclic and monotonic performance of unstiffened extended end-plate connections having thin end-plates and large-bolts. Engineering Structures, 2023. 281: p. 115794.
[22]. ABAQUS, ABAQUS/Standard User's Manual, 2020th ed. ABAQUS/Standard User's Manual, 2020th ed, ed. D.S.S. Corp. 2020: Dassault Systèmes Simulia Corp.

[23]. Haghollahi, A. and R. Jannesar, Cyclic behavior of bolted extended end-plate moment connections with different sizes of end plate and bolt stiffened by a rib plate. Civil Engineering Journal, 2018. 4(1): p. 200-211.
[24]. Tartaglia, R., et al. Finite element analyses on seismic response of partial strength extended stiffened joints. in COMPDYN 2017-Proceedings of the 6th International Conference on Computational Methods in Structural Dynamics and Earthquake Engineering. 2017.
[25]. CEN, EN 1993-1-8, Eurocode 3, in Design of Steel Structures, Part 1-8: Design of Joints. 2012, European Committee for Standardization: Brussels, Belgium.